

## *Retraction*

# **Retracted: Nanoscale Characterization and Impurities of Fused Silica Optical Surfaces**

### **Advances in Materials Science and Engineering**

Received 26 December 2023; Accepted 26 December 2023; Published 29 December 2023

Copyright © 2023 Advances in Materials Science and Engineering. This is an open access article distributed under the Creative Commons Attribution License, which permits unrestricted use, distribution, and reproduction in any medium, provided the original work is properly cited.

This article has been retracted by Hindawi, as publisher, following an investigation undertaken by the publisher [1]. This investigation has uncovered evidence of systematic manipulation of the publication and peer-review process. We cannot, therefore, vouch for the reliability or integrity of this article.

Please note that this notice is intended solely to alert readers that the peer-review process of this article has been compromised.

Wiley and Hindawi regret that the usual quality checks did not identify these issues before publication and have since put additional measures in place to safeguard research integrity.

We wish to credit our Research Integrity and Research Publishing teams and anonymous and named external researchers and research integrity experts for contributing to this investigation.

The corresponding author, as the representative of all authors, has been given the opportunity to register their agreement or disagreement to this retraction. We have kept a record of any response received.

### **References**

- [1] Z. Dai, S. Zhou, Z. Huang, and H. Li, "Nanoscale Characterization and Impurities of Fused Silica Optical Surfaces," *Advances in Materials Science and Engineering*, vol. 2022, Article ID 8308746, 8 pages, 2022.

## Research Article

# Nanoscale Characterization and Impurities of Fused Silica Optical Surfaces

Zuocai Dai <sup>1,2</sup>, Sha Zhou,<sup>3</sup> Zhiliang Huang,<sup>1,2</sup> and Hao Li<sup>1</sup>

<sup>1</sup>College of Mechanical and Electrical Engineering, Hunan City University, Yiyang 413002, Hunan, China

<sup>2</sup>Key Laboratory Energy Monitoring and Edge Computing for Smart City of Hunan Province, Yiyang 413002, Hunan, China

<sup>3</sup>Hunan City University, Yiyang 413002, Hunan, China

Correspondence should be addressed to Zuocai Dai; [daizuocai@hncu.edu.cn](mailto:daizuocai@hncu.edu.cn)

Received 12 May 2022; Revised 8 June 2022; Accepted 15 June 2022; Published 16 July 2022

Academic Editor: Haichang Zhang

Copyright © 2022 Zuocai Dai et al. This is an open access article distributed under the Creative Commons Attribution License, which permits unrestricted use, distribution, and reproduction in any medium, provided the original work is properly cited.

Fused silica is produced by melting high-purity silica and then rapidly cooling it. It has good physical and chemical properties, which also make it the raw material for most components in the optical industry, and is widely used in optical fiber communications, semiconductors, and aerospace. The content of SiO<sub>2</sub> in fused silica is as high as 99.995% or more, but some impurities will still be generated during production and processing. The impurity elements of its optical curved surface can induce damage to the fused silica and adversely affect its performance, thereby affecting the performance of the fabricated element. In this paper, the impurities in the nanostructure of the fused silica optical surface are mainly analyzed, and the impurities on the surface are qualitatively and quantitatively analyzed by the characterization methods of secondary ion mass spectrometry (SIMS) and X-ray diffraction analysis, respectively. The main component type and content of impurities were measured. The experimental results have an important impact on the production and preparation of optical components using fused silica as raw materials, which can remove surface impurities in a targeted manner and better utilize the advantages of fused silica materials.

## 1. Introduction

Fused silica has the advantages of high temperature resistance, corrosion resistance, strong light transmission, low expansion coefficient, and good insulation. It has the reputation of “glass king” and is widely used in high-tech fields. The raw material of fused quartz is generally natural crystal, its main component is silicon dioxide, and the content of SiO<sub>2</sub> is as high as 99.995%~99.998%. Fused quartz, as the name suggests, is a material made of quartz as raw material, which is melted at a high temperature of about 2000°C and then rapidly cooled. Due to the purity of the raw material, the melting process, and processing, there will still be some impurities on the surface. The purity of the quartz raw material is relatively high, so that the content of these impurities is extremely low, and most of them are nanoscale. Different impurities will affect the high temperature resistance, light transmission, and insulation properties of fused silica to varying degrees, thereby affecting the performance

of the fabricated device and adversely affecting the precision of the final instrument. Therefore, the nanoscale impurity analysis of fused silica optical surfaces is very necessary.

The application fields of fused silica materials are very wide, impurities will adversely affect material properties, and the requirements for the purity of fused silica are also getting higher and higher. It is necessary to characterize and analyze the impurities on its optical surface, and many scholars have also studied it. Rogers et al. gave an overview of the production status of silicon products, analyzed the reaction of hot silicon and hot carbon in electric furnaces, and introduced the production method of fused silica [1]. Leonov studied the effect of laser ablation on the properties of metal impurities on the surface of fused silica and obtained the elimination and absorption spectra and difference spectra of silica and coated substrates [2]. Feng et al. proposed that fused silica contains impurities Fe and Ce, and these metal impurities will induce damage to fused silica under laser irradiation, and the light transmittance will also decrease [3].

Based on the Mie theory and thermal equation, combined with the measurement of the main components of impurities on the surface of fused silica by ICP-OES, Xiang et al. analyzed the laser damage probability of Cu, Al, and  $\text{CeO}_2$  on fused silica by three impurities [4]. Arosa and de la Fuente proposed the use of low coherence interferometry to measure material dispersion in fused silica, which can be used to measure impurities in fused silica materials quickly and efficiently over a wide spectral range [5]. Shuhao et al. studied the surface structure characteristics of laser-induced microplasma on fused silica and measured the intensity of its microplasma and found that the microplasma was related to the ablation of fused silica [6]. Hongjie et al. believed that the laser-induced damage on the fused silica surface is often ignited by absorbing impurities introduced by the polishing process. They analyzed the laser damage mechanism of Fe and Ce impurities on the surface of fused silica and carried out surface impurity analysis, photothermal absorption analysis, and fog damage mechanism analysis. The results showed that both Ce and Fe impurities on the surface have serious effects on the laser-induced intrinsic damage [7]. These scholars basically study the damage of impurities on the surface of fused silica by laser and have not conducted in-depth research at the nanometer level.

Kunz et al. proposed a method to achieve reproducible direct writing of subwavelength nanostructures on fused silica based on LIPSS laser energy, promoting the development of nanoscale optical materials [8]. Kotz et al. mainly introduced a kind of solid nanocomposite Glassomer prepared at submicron resolution by polymer molding and subtraction technology, which can be transformed into optical nanoscale fused silica glass after heat treatment [9]. Park et al. have advanced fused silica nanoscale research by developing a fabrication process for 120 nm wide fused silica "nanowalls" with high aspect ratios using fluorine-based deep reactive ion etching [10]. Wang et al. mainly used nanoscale fluorescent quantum dot technology to mark defects on the surface of optical components and quantitatively characterized the damage degree of fused silica surface through the change of fluorescence quantum intensity. The results showed that the nanoscale quantum dot technology can annotate the surface defects of optical components [11]. Jiang et al. investigated the change of surface nanoroughness during inductively coupled plasma etching of fused silica through experiments and proposed a theoretical model based on the change of surface morphology. The etched surface is biscal at the beginning, and the surface peaks are rougher than the surface valleys; when the surface topography is transformed to a single scale, the surface peak-valley roughening process slows down [12]. These scholars studied the nanoscale structure of fused silica but did not analyze its nanoscale impurities.

However, most of the research works of these scholars are about the influence of fused silica surface impurities on the surface laser damage of fused silica or the nanoscale structure and surface nanoroughness of fused silica. Regarding analysis of these two aspects, there is no qualitative and quantitative analysis specifically for nanoscale impurities in optical surfaces. The existence of some impurities on

the surface of fused silica has a great influence on the performance of components with fused silica as the main raw material. It is of great significance to study the nanoscale impurities on the optical surface of fused silica. Therefore, this paper mainly studies the nanoscale impurities on the fused silica optical surface. The characterization methods used are mainly SIMS and X-ray diffraction technology.

## 2. Fused Silica Nanoscale Optical Surface Structure

*2.1. Fused Silica Structure.* Fused silica, also known as quartz glass, is actually obtained by subjecting high-purity quartz to a high-temperature melting process followed by rapid cooling, which is also a kind of glass. Basically, there is only one component of silica, and the composition is single. Therefore, it has many excellent properties different from glass. It is mostly used to make optical components and is widely used in industrial manufacturing.

The raw material of fused quartz is natural quartz, which has a relatively high purity and a small number of impurities. The main component of quartz is silicon dioxide. From the perspective of microstructure, quartz crystal is a network space structure surrounded by silicon atoms and oxygen atoms. The ratio of silicon atoms to oxygen atoms is 1 : 2. Among them, the bond length of the silicon-oxygen bond and the diameter of the silicon atom and the oxygen atom are all nanoscale, and the length of the silicon-oxygen bond is 0.162 nm. Quartz crystal structure arrangement is relatively regular, and the structure is shown in Figure 1.

The structure of fused silica is roughly similar to that of quartz crystal, but there are some deviations locally, mainly because the length of the silicon-oxygen bond has changed after the quartz is melted at high temperature. On the whole, the arrangement of the fused quartz crystal structure is not as regular as that of the quartz crystal, so it will appear isotropic on the macroscopic level. From the perspective of microstructure, fused silica is composed of many silicon dioxide tetrahedral structural units of the same species, but, due to the high temperature during the melting process, the silicon-oxygen bond is shortened compared with quartz crystal, and the bond length is only 0.155 nm. It is precisely because the chemical bond energy of the Si-O bond is large and the structural network is highly compact that fused silica has good physical and chemical properties that are different from those of quartz crystals. The increase of chemical bond energy also improves the stability of the fused silica structure. The structure of fused silica is shown in Figure 2.

*2.2. Nanoscale Structure.* Nanostructures are structures of objects with dimensions between molecular and micrometer scales, typically below 100 nm in size. In nanomaterials, most of them are composed of nonmetallic elements, of which carbon is the most widely used element, which is an essential component of organic compounds; next is silicon, which is mostly used in semiconductor materials. Silicon in nature is mostly in the form of oxide silicon dioxide, and nanoscale silicon dioxide materials are an important part of the

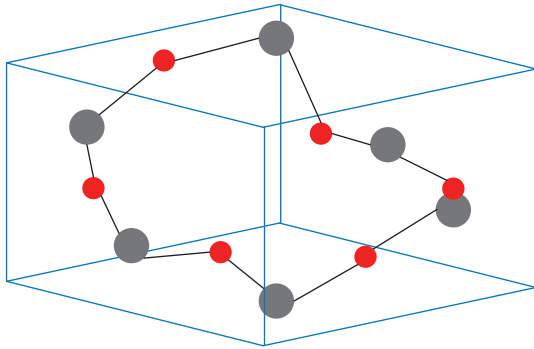


FIGURE 1: Quartz crystal structure.

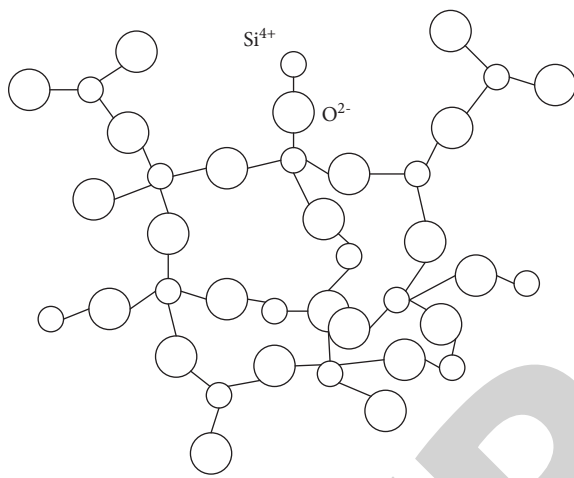


FIGURE 2: Fused silica structure.

manufacture of most optical components. Technology has been developing, and process manufacturing has higher requirements for the precision of materials and instruments, but traditional micron-scale structures have been unable to meet research needs. Therefore, chemists and materials scientists are exploring more and more nanoscale fused silica, nanoscale materials play an increasingly important role, and their application fields are becoming more and more extensive.

The bond length of the silicon-oxygen bond in the nanoscale structure of fused silica is 0.155 nm, the overall particle size is also below 0.3  $\mu\text{m}$ , and the structural network is very closely arranged. Nanoscale fused silica has the characteristics of small particle size, large surface area, good biocompatibility, and so forth. It can be involved in almost all industries that use silica materials and has strong optical and industrial application prospects [13]. Not only can nanofused silica be used as a raw material for the manufacture and processing of components, but also it can be added to other materials in proportion according to actual needs by using its special structure and properties. It can be made into composite materials that meet the actual needs of production and processing and provide more possibilities for the development of new components. For example, carbon is added to fused silica, and the resulting composite material plays an important role in missile communication, guidance, and heat protection.

### 3. Fused Silica Optical Surface Impurity Method

For the impurity analysis of the fused silica optical surface, the main purpose is to measure the type and content of impurities. Therefore, the analysis should be carried out from the qualitative and quantitative aspects. In the process of fused silica impurity determination, there are many methods that can be used. On the premise of considering the characteristics of fused silica and ensuring the accuracy of the experimental results, this paper mainly uses SIMS to qualitatively analyze the types of impurities. The quantitative analysis method is the X-ray diffraction technique.

**3.1. Secondary Ion Mass Spectrometry.** SIMS (secondary ion mass spectroscopy) is a sensitive technique for detecting compositional information on solid surfaces and near surfaces [14]. The technical principle is to use a certain high-energy primary ion beam incident on the surface of the sample. The high energy is generally keV or MeV level, and the beam energy exceeds the threshold of the bombarded material surface to generate secondary ions. During this process, some of the ions are backscattered and bounced outward, while others enter the interior of the sample and collide with particles on the surface of the sample. When these particles reach the scattering threshold energy, they are excited to eject. Some of the sputtered particles have positive and negative charges. These secondary ions first enter the energy analyzer, then enter the mass analyzer to record the mass-to-charge ratio of the ions, and finally obtain the mass spectrum of the relevant elements through the ion detector. The detailed explanation is shown in Figure 3.

Time-of-flight SIMS can analyze impurities in a large mass range and high resolution, improving the utilization of samples and the accuracy of detection. A time-of-flight mass analyzer is a pseudosynchronous type detection device that can be accurate to the microsecond level, and it can complete a complete mass spectrometry detection in about 30 microseconds. In the time-of-flight SIMS analysis, a Ga, Cs, or Ar ion source with an ion beam energy of 25 keV is generally used to bombard the test area of 200  $\mu\text{m} \times 200 \mu\text{m}$  on the surface, and the ion sputtering in the range of 20  $\mu\text{m} \times 20 \mu\text{m}$  is mainly analyzed. The secondary ion mass spectrum is obtained by the ion detector, the mass-to-charge ratio of the ions is analyzed, the data with the highest relative intensity is found, and the type of impurity element is finally analyzed. Secondary ions are formed after the primary ion beam bombards the sample surface. Secondary ions are accelerated in an electric field as they pass through the energy analyzer, and each ion acquires the same initial kinetic energy in the same electric field. These ions then fly into the field-free region, the drift tube. In the case of the same initial kinetic energy, ions with different mass-to-charge ratios obtain different velocities, and most ions do parabolic motion in the electric field. The kinetic energy acquired by each ion is determined by the charge ( $q$ ) of the ion, the potential difference ( $E$ ) of the electric field, and the distance ( $s$ ). Then the kinetic energy after acceleration is expressed by ion mass ( $m$ ) and ion velocity ( $v$ ) as

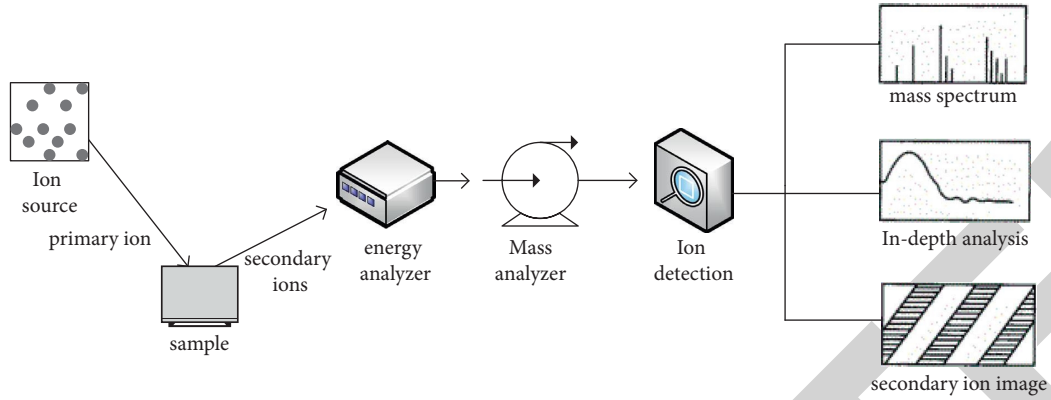


FIGURE 3: Principles of secondary ion mass spectrometry.

$$\frac{1}{2}mv^2 = qEs, \quad (1)$$

where  $D$  represents the distance the ion flies before reaching the detector, which is also known from the displacement formula:

$$D = vt_d. \quad (2)$$

After arranging equations (1) and (2), the time  $t_d$  for ions to fly through the drift tube can be expressed as

$$t_d = D\sqrt{\left(\frac{m}{2qEs}\right)}. \quad (3)$$

The formula for the mass-to-charge ratio  $m/q$  can be obtained as

$$\sqrt{\left(\frac{m}{q}\right)} = \frac{\sqrt{2Es}}{D}t_d. \quad (4)$$

It can be seen from formula (4) that, in the same electric field, the mass-to-charge ratio of ions is mainly related to the distance  $s$ , time  $t_d$ , and displacement  $D$ . Under bombardment of the same energy, each ion has the same initial kinetic energy. From the kinetic energy formula (1), it can be known that the flight speed of different ions is different, the natural flight path is different, and the time to reach the end point is also different. Finally, the mass spectrum of each secondary ion is obtained, and the composition of the substance is analyzed from the mass spectrum; that is, the qualitative analysis is completed.

**3.2. X-Ray Diffraction Technology.** X-rays are a type of electromagnetic wave. The basic principle of diffraction is that when X-rays are incident on a crystal, the distances between these atoms are of the same order of magnitude as the wavelength of the incident X-rays, so X-rays scattered by different atoms interfere with each other. Diffraction lines are generated in certain directions, and the orientation and intensity of the diffraction lines are spatially distributed [15]. XRD is mainly suitable for phase analysis and quantitative analysis of crystalline substances [16]. In the qualitative analysis, compare the diffractogram of the sample with the

standard diffraction card; in the quantitative analysis: calculate by analyzing the diffraction intensity data of the sample.

**3.2.1. Basic Composition of X-Ray Diffractometer.** The X-ray diffractometer consists of five parts, namely, highly stable X-ray source, sample and sample position adjustment system, diffraction detector, instrument measurement and recording system to obtain diffraction pattern, and diffraction pattern processing and analysis system. In the X-ray diffraction experiment, the X-ray diffractometer can basically achieve no damage to the sample, high efficiency and speed, and high measurement accuracy in the experimental results, and the obtained information integrity is also high, as shown in Figure 4.

**3.2.2. Bragg Equation.** The Bragg equation reflects the relationship between the direction of the diffraction line and the crystal structure and is the basic condition that X-ray diffraction needs to meet [17]. Generally, X-rays of known wavelength are used to irradiate an unknown crystal, and the interlayer spacing  $d$  in the crystal is obtained by measuring the diffraction angle.

Two X-rays emitted by the same point light source  $S$  are reflected to  $S_1$  by different crystal planes, as shown in Figure 5.

The optical paths of the two rays are

$$n\lambda = 2d \sin \theta. \quad (5)$$

Formula (6) is the Bragg equation, where  $\theta$  is the incident angle,  $d$  is the interplanar spacing,  $n$  is the diffraction order,  $\lambda$  is the incident ray wavelength, and  $2\theta$  is the diffraction angle. In addition to the diffraction experiments of crystals, the Bragg equation can also be extended to the study of polymer structures.

Let the wavelength of monochromatic light with frequency  $\nu$  be  $\lambda$  when it propagates in vacuum, and the propagation speed is  $c$ ; then the speed formula is

$$c = \lambda\nu. \quad (6)$$

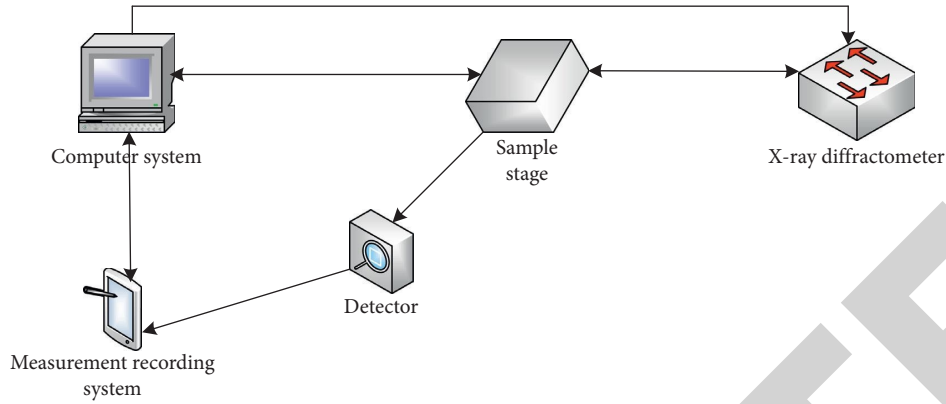


FIGURE 4: Basic structure of X-ray diffractometer.

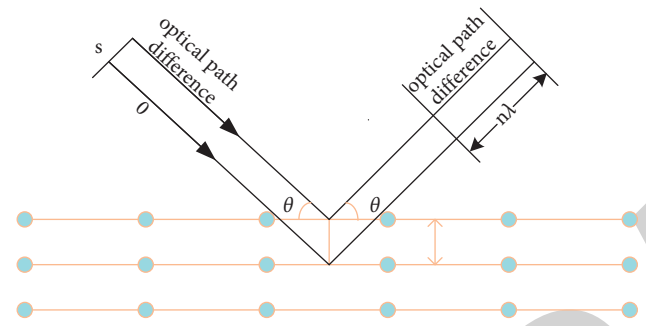


FIGURE 5: Relationship between diffraction line orientation and crystal structure.

If the propagation velocity of monochromatic light is  $u$  in a medium with a refractive index of  $n$ , we can get

$$u = \frac{c}{n}. \quad (7)$$

Through the above formula, the wavelength in this medium can be obtained as

$$\lambda' = \frac{u}{\nu} = \frac{c}{n\nu} = \frac{\lambda}{n}. \quad (8)$$

A conclusion can be drawn from formula (9): when monochromatic light propagates in a medium with a refractive index of  $n$ , its wavelength is  $(1/n)$  times that of its propagation wavelength in vacuum.

If light travels a distance  $r$  in a medium, its phase change is

$$\Delta\phi = 2\pi \frac{r}{\lambda'} = 2\pi \frac{nr}{\lambda}. \quad (9)$$

According to formula (10), it can be known that the product of the geometric distance  $r$  of the monochromatic light propagating in the medium and the refractive index  $n$  of the medium is fixed. According to the actual calculation needs, this fixed value can be defined as the optical distance, the distance the light travels in the vacuum in the same time, which is expressed by the following formula:

$$\Delta = nr. \quad (10)$$

When monochromatic light passes through several different media continuously, its optical path is

$$\Delta = \sum_i n_i r_i. \quad (11)$$

With the introduction of the optical path concept, there is no need to do special calculations on the phase changes caused by the propagation of light in different media, and the optical path formula can be directly introduced, which provides great convenience for the application of the Bragg equation.

**3.2.3. Scherrer Formula.** The Scherrer formula is the theoretical basis for measuring grain size, which describes the relationship between the grain size and the half-width of the diffraction peak [18]. The diffraction pattern obtained according to the Scherrer formula reflects the size of the crystal grains, and the structure of the unknown substance can be analyzed. The specific formula is as follows:

$$D = \frac{K\lambda}{B \cos \theta'} \quad (12)$$

where  $K$  is the Scherrer constant, and its value is 0.89;  $D$  is the grain size, generally in nanometers;  $B$  is the half-height width of the diffraction peak, which needs to be converted into radians (rad) when calculating.

**3.2.4. Quantitative Analysis of the Phase.** Quantitative phase analysis is mainly based on the relative intensity of diffraction lines and phase content and data analysis [19]. The intensity of the diffraction line increases with the increase of the phase content, and the phase content can be calculated according to the intensity of the diffraction line through the relevant formula. Many substances and materials have more or less impurities, and there are very few pure substances. In order to analyze the content of impurities from a quantitative point of view, it is necessary to perform data processing with the help of phase quantitative formulas.

Assuming that the sample is a mixture composed of  $n$  phases and the line absorption coefficient is  $\mu$ , the crystal plane diffraction line intensity of phase  $i$  is

$$I_i = I_0 \cdot \frac{\lambda^3}{32\pi R} \cdot \left( \frac{e^2}{mc^2} \right) \cdot \frac{1}{2\mu} \cdot \left[ \frac{V}{V_0^2} \cdot P \cdot F_{HKL}^2 \cdot \frac{1 + \cos^2 2\theta}{\sin^2 \theta \cos \theta} \cdot e^{-2M} \right]. \quad (13)$$

If the volume fraction of phase  $i$  is  $f_i$  and the volume  $V$  of the sample being irradiated is the unit volume, there are

$$V_i = V \cdot f_i = f_i. \quad (14)$$

When the content of phase  $i$  is changed, in formula (13), except  $f_i$  and  $\mu$ , all others are regarded as constants, which are combined and denoted as  $C_i$ . Then, the relative cumulative intensity  $I_i$  of a diffraction line of phase  $i$  is

$$I_i = \frac{C_i V_i}{\mu} = \frac{C_i f_i}{\mu}. \quad (15)$$

The content is expressed in mass fraction:

$$x_i = \frac{V_i \cdot \rho_i}{V \cdot \rho} = f_i \cdot \frac{\rho_i}{\rho}. \quad (16)$$

The mass absorption coefficient is

$$I_i = \frac{C_i x_i}{\rho_i \mu_m}. \quad (17)$$

X-ray diffraction technology is a method used for quantitative analysis of impurities in many materials, which can solve the problem that SIMS cannot quantitatively analyze impurities on fused silica optical surfaces. This method can directly measure the mass fraction of impurities; the limitation is that it needs to be further converted into the content of impurities in the sample through the formula.

#### 4. Fused Silica Optical Surface Impurity Experiment

Sample selection was as follows: four pieces were cut from the same fused silica material and chemically mechanically polished to become fused silica substrates. The size of the sample is  $2 \text{ mm} \times 2 \text{ mm}$  and the thickness is  $5 \text{ mm}$ . The mass of each block was weighed with a microelectronic balance and numbered as sample 1, sample 2, sample 3, and sample 4, respectively. When taking samples, ensure that the samples are clean and do not touch the area to be tested. After sampling, the samples were kept in a vacuum environment to avoid foreign contamination affecting the final experimental results.

In the impurity analysis of the fused silica optical surface, the characterization methods used are SIMS and X-ray diffraction to analyze the surface impurity characteristics of the fused silica. These two methods can, respectively, measure the type and content of impurities in the fused silica optical surface. Finally, the results of the two experiments should be summarized.

**4.1. Secondary Ion Mass Spectrometry Analysis.** Experimental procedure was as follows: a Ga ion source with a beam energy of  $28 \text{ keV}$  was used to bombard the test area of  $200 \mu\text{m} \times 200 \mu\text{m}$  on the surface of sample 1 to generate secondary ions, and the excited secondary ions flew freely into the energy analyzer and mass analyzer. By observing the flight path of the ions, it measures the flight distance and flight time of each secondary ion in the process and mainly

analyzes the range of  $20 \mu\text{m} \times 20 \mu\text{m}$  to improve the accuracy. According to the distribution curve of sputtering ion yield of these impurity elements with sputtering time, the mass spectrum of impurity ions with respect to relative abundance and mass-to-charge ratio can be obtained. In the final experiment, a clear mass spectrum was selected for analysis, and the mass-to-charge ratio with a relative intensity of 100% was taken and compared with the standard mass-to-charge ratio. Bing analyzed the type of impurities contained on the surface of fused silica according to the mass-to-charge ratio.

In the mass spectrum, the abscissa represents the mass-to-charge ratio of ions, which gradually increases from left to right; the ordinate represents the intensity of the ion current, and the intensity of the strongest ion current is set as 100%, and the intensity of other ion currents is expressed as a percentage [20]. Various elements usually exist in various forms in nature, such as elemental substances, compounds, or charged free states, and sometimes ions have several valence states. Therefore, the mass-to-charge ratio obtained in the mass spectrum is not a single value but different values. If you want to measure what the impurity substance actually exists on the fused silica optical surface, you must select the one with the highest relative intensity. The time-of-flight secondary ion mass spectrometer has certain defects in practical application. Impurities can only be calculated and analyzed based on the mass-to-charge ratio of the obtained mass spectrum. It is not possible to calibrate and analyze the impurity elements in fused silica, so it is impossible to calculate the content of impurities. Generally, only qualitative analysis is performed.

**4.2. X-Ray Diffraction.** Samples 2, 3, and 4 that were sampled in advance were ground into powders, placed on the sample stage, filled into the sample holder in turn, and diffracted by the X-ray generator. In order to reduce the experimental error caused by accidental factors or improper operation, three identical experiments were carried out for three samples. When the goniometer is measuring, the value of the 2-theta diffraction angle can be measured, and then the goniometer and the detector of the X-ray diffractometer are connected. After setting the parameters, the results detected by the detector will be displayed on the application software. The results of the test will be input to the measurement recording system and finally input in the computer system to obtain the diffraction image of the impurity with respect to the diffraction angle and intensity data.

According to the diffractogram obtained from the above experiments, the goniometer and X-ray diffractometer can obtain the diffraction angle and diffraction intensity data of the sample, conduct analysis, and calculate the impurity content [21]. The mass absorption coefficient was calculated from the relative cumulative intensity of diffraction, and the final impurity content was calculated as the representative content of mass fraction. There are many impurities in fused silica, and some impurities are extremely small. The data of the main impurity elements obtained in the SIMS experiment can be used. In this experiment, the main elements are

TABLE 1: Impurity content of three samples of fused silica optical surfaces.

Type	Content ( $\mu\text{g/g}$ )		
	Sample 1	Sample 2	Sample 3
Al	13.9	14.2	14.5
Ce	1.3	1.4	1.2
Fe	1.3	1.2	1.1
Cu	0.6	0.5	0.7

calibrated and analyzed. According to the data of various impurities reflected in the diffractogram, the relative concentration of impurities can be measured by formula, and the content of various impurities can be finally calculated.

## 5. Fused Silica Optical Surface Impurity Results

The impurities in the fused silica optical surface were qualitatively analyzed by the experiment of SIMS. According to the obtained mass spectrum, in this paper, the types of various impurities existing on the surface are analyzed, and then the phase quantitative analysis is carried out through X-ray diffraction experiments, and the content of various impurities in fused silica is calculated according to the relevant formula. These two characterization methods from different angles can basically complete the experiment of impurity determination and obtain the experimental results.

In the SIMS experiment, the secondary ion mass spectrum of the corresponding element can be obtained according to the detection of the sample by the time-of-flight mass spectrometer. The mass-to-charge ratio can be obtained from the mass spectrum, and the one with the highest relative intensity can be found and analyzed one by one, combining multiple factors to find the impurity composition on the surface. There are many impurities in quartz sand, but extremely trace elements can be ignored. In this experiment, only the four ion sputtering yields in the spectrum are selected for analysis. The experimental results showed that the impurity elements of the fused silica optical surface are mainly Al, Ce, Fe, and Cu and generally exist in the form of oxides on the surface.

In the X-ray diffraction experiment, the data of the diffraction angle and the diffraction line intensity can be obtained according to the diffractogram, which can be substituted into the formula to calculate the final impurity content with the mass fraction representing the content. Since the content of impurities in fused silica is relatively small, it is convenient for statistics and calculation after the unit conversion of the content of the main impurities. Therefore, the unit of impurity content is set to  $\mu\text{g/g}$ ; that is, how much does each gram of fused silica contain micrograms of impurities? The contents of main impurities in sample 2, sample 3, and sample 4 are shown in Table 1.

In the process of quantitative analysis of impurities, one-time results are often inaccurate and may be affected by accidental factors. Therefore, in order to reduce the experimental error and obtain experimental data closer to the actual situation, a total of three quantitative analysis experiments were carried out, and the average value of the

TABLE 2: Impurity content of fused silica optical surface.

Type	Al	Ce	Fe	Cu
Content ( $\mu\text{g/g}$ )	14.2	1.3	1.2	0.6

impurity content in the three experimental results was taken. After averaging the data in Table 1, the final results are obtained, as shown in Table 2.

## 6. Conclusion

This paper introduces the structure of fused silica, the causes of its excellent physical and chemical properties, and the wide application of nanoscale fused silica materials in various fields. The nanoscale impurities on the surface were qualitatively and quantitatively analyzed by SIMS and X-ray diffraction, respectively, and the types and contents of nanoscale impurities on the fused silica optical surface were analyzed. The experimental results show that the impurity elements of the fused silica optical surface are Al, Ce, Fe, and Cu, among which the content of Al is  $14.2 \mu\text{g/g}$ , the content of Ce is  $1.3 \mu\text{g/g}$ , the content of Fe is  $1.2 \mu\text{g/g}$ , and the content of Cu was  $0.6 \mu\text{g/g}$ . The content of Al element is the highest, because Al element is distributed in natural quartz, the raw material of fused silica. These impurities will destroy the chemical bonds and other structures of the fused silica itself, thereby affecting the chemical properties. The results of this experiment have an impact on the production and preparation of optical components using fused silica as raw material. Physical or chemical methods can be used to remove surface impurities in a targeted manner to reduce the damage of impurities to fused silica, so as to better utilize the advantages of fused silica as an optical and industrial material.

## Data Availability

No data were used to support this study.

## Conflicts of Interest

The authors declare that the research was conducted in the absence of any commercial or financial relationships that could be construed as potential conflicts of interest.

## Acknowledgments

This work was supported by the Project of Natural Science Foundation of Hunan Province (2021JJ40027) and the Scientific Research Project of Hunan Education Department (20B113).

## References

- [1] B. A. Rogers, W. J. Kroll, and H. P. Holmes, "Production of fused silica," *Transactions of the Electrochemical Society*, vol. 92, no. 1, pp. 413–424, 2019.
- [2] N. B. Leonov, "Influence of adsorbed metal atoms on light absorption by a fused silica surface," *Optics and Spectroscopy*, vol. 128, no. 12, pp. 2046–2049, 2020.



- [3] Q. Feng, L. Li, T. Zeng et al., "Ab initio molecular dynamics simulation of the effect of impurities on laser-induced damage of fused silica," *Physica B: Condensed Matter*, vol. 545, pp. 549–558, 2018.
- [4] G. Xiang, G. Feng, and L. Zhai, "Effect of subsurface impurities of fused silica on laser-induced damage probability," *Infrared and Laser Engineering*, vol. 46, no. 04, pp. 30–35, 2017.
- [5] Y. Arosa and R. De la Fuente, "Refractive index spectroscopy and material dispersion in fused silica glass," *Optics Letters*, vol. 45, no. 15, 4268 pages, 2020.
- [6] C. Shuhao, V. Rymkevich, M. Sergeev, and A. Samokhvalov, "Features of fused silica ablation by laser induced carbon microplasma," *Optical and Quantum Electronics*, vol. 52, no. 2, 118 pages, 2020.
- [7] L. Hongjie, W. Fengrui, H. Jin et al., "Experimental study of 355 nm laser damage ignited by Fe and Ce impurities on fused silica surface," *Optical Materials*, vol. 95, Article ID 109231, 2019.
- [8] C. Kunz, S. Engel, F. A. Müller, and S. Gräf, "Large-area fabrication of laser-induced periodic surface structures on fused silica using thin gold layers," *Nanomaterials*, vol. 10, no. 6, 1187 pages, 2020.
- [9] F. Kotz, N. Schneider, A. Striegel et al., "Glassomer-processing fused silica glass like a polymer," *Advanced Materials*, vol. 30, no. 22, Article ID 1707100, 2018.
- [10] J.-R. Park, A. Berndt, Y. K. Kim, J. S. Lee, J. E. Ryu, and D. S. Choi, "Formation of high aspect ratio fused silica nanowalls by fluorine-based deep reactive ion etching," *Nano-Structures & Nano-Objects*, vol. 15, pp. 212–215, 2018.
- [11] H. X. Wang, J. Hou, J. H. Wang, B. W. Zhu, and Y. H. Zhang, "Experimental investigation of subsurface damage depth of lapped optics by fluorescent method," *Journal of Central South University*, vol. 25, no. 7, pp. 1678–1689, 2018.
- [12] X. Jiang, L. Zhang, Y. Bai et al., "Bi-stage time evolution of nano-morphology on inductively coupled plasma etched fused silica surface caused by surface morphological transformation," *Applied Surface Science*, vol. 409, pp. 156–163, 2017.
- [13] Y. Liu, D. Hirsch, R. Fechner et al., "Nanostructures on fused silica surfaces produced by ion beam sputtering with Al co-deposition," *Applied Physics A*, vol. 124, no. 1, 73 pages, 2018.
- [14] K. Wu, F. Jia, W. Zheng, Q. Luo, Y. Zhao, and F. Wang, "Visualization of metalodrugs in single cells by secondary ion mass spectrometry imaging," *JBIC, Journal of Biological Inorganic Chemistry*, vol. 22, no. 5, pp. 653–661, 2017.
- [15] J. Filik, A. W. Ashton, P. C. Y. Chang et al., "Processing two-dimensional X-ray diffraction and small-angle scattering data inDAWN 2," *Journal of Applied Crystallography*, vol. 50, no. 3, pp. 959–966, 2017.
- [16] T. Toraya, "A new method for quantitative phase analysis using X-ray powder diffraction: direct derivation of weight fractions from observed integrated intensities and chemical compositions of individual phases. Corrigendum," *Journal of Applied Crystallography*, vol. 50, no. 2, 665 pages, 2017.
- [17] S. Rabaste, J. Bellessa, A. Brioude et al., "Sol-gel fabrication of thick multilayers applied to Bragg reflectors and micro-cavities," *Thin Solid Films*, vol. 416, no. 1-2, pp. 242–247, 2002.
- [18] M. Rabiei, A. Palevicius, A. Monshi, S. Nasiri, A. Vilkauskas, and G. Janusas, "Comparing methods for calculating nano crystal size of natural hydroxyapatite using X-ray diffraction," *Nanomaterials*, vol. 10, no. 9, 1627 pages, 2020.
- [19] A. Neumann, M. Klinkenberg, and H. Curtius, "Corrosion of non-irradiated UAlx-Al fuel in the presence of clay pore solution: a quantitative XRD secondary phase analysis applying the DDM method," *Radiochimica Acta*, vol. 105, no. 2, pp. 85–94, 2017.
- [20] W. Li, R. Li, H. Liu et al., "A comparison of liquid chromatography-tandem mass spectrometry (LC-MS/MS) and enzyme-multiplied immunoassay technique (EMIT) for the determination of the cyclosporin A concentration in whole blood from Chinese patients," *BioScience Trends*, vol. 11, no. 4, pp. 475–482, 2017.
- [21] B. Hwang, T. Woo, and J. H. Park, "Fast diffraction-limited image recovery through turbulence via subsampled bispectrum analysis," *Optics Letters*, vol. 44, no. 24, 5985 pages, 2019.